

# Preliminary investigation on integration of semi-active structural control and earthquake early warning

Iervolino I., Galasso C., Manfredi G.

Dipartimento di Ingegneria Strutturale, Università degli Studi di Napoli Federico II  
 via Claudio 21, 80125 Naples, Italy  
 eMail: lunio.iervolino@unina.it, carmine.galasso@unina.it, gaetano.manfredi@unina.it

## 1. Introduction

Earthquake Early Warning Systems (EWS) are tools for real-time seismic risk management. EWS potentially enable different possible risk mitigation actions, to be carried out when an alarm is issued, depending on the amount of lead-time available (defined as the warning time between the alarm and the strike at the site of interest). Examples of such actions, classified according to the lead-time required to be undertaken, are reported in Figure 1 for the Campania region (southern Italy) which is provided with a regional EWS, the Irpinia Seismic Network (ISNet) comprised of 29 seis-

mic stations with real-time capabilities (Weber et al., 2007).

In epicentral areas, only a few seconds of warning time is available, and an EWS can only be used to trigger automated decision and risk mitigation procedures (i.e., the lead-time is too short to allow for manned operations). This is the case, for example, of the Campania region where the most hazardous seismogenetic sources zone is close to densely urbanized areas and time-consuming security actions, as evacuation, may be unfeasible.

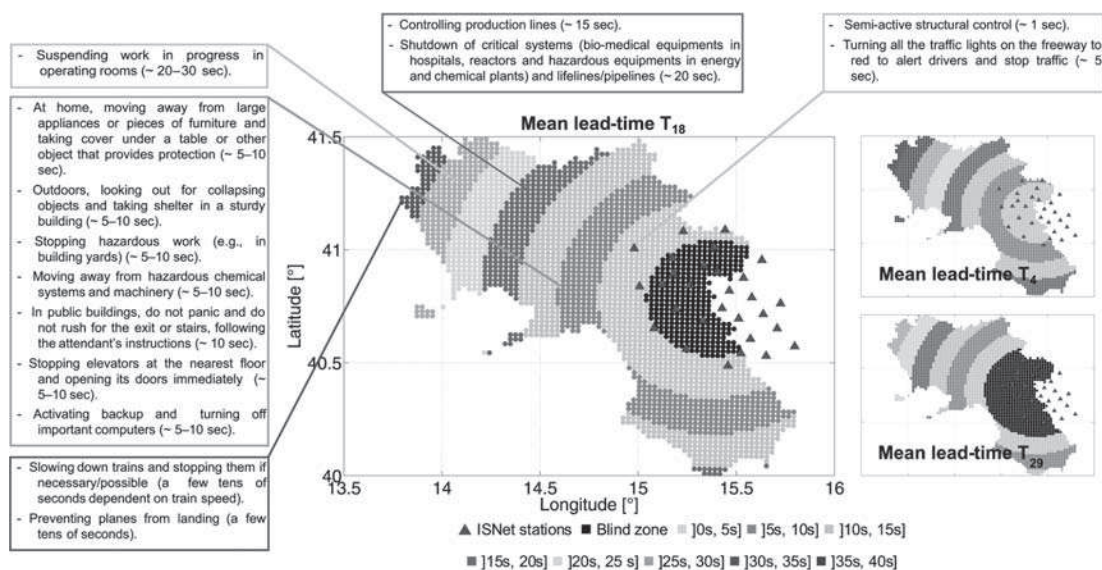


Figure 1: Information-dependent lead-time maps for the Campania (southern Italy) region and possible risk reduction actions (Iervolino et al., 2009)

Some studies discuss, as an engineering application of EEW, especially in areas where the available lead-time is low, the semi-active control of structures; i.e., the building can change its dynamic properties within a few seconds (or milliseconds) to better withstand the impending ground motion (Pnevmatikos et al., 2004; Occhiuzzi et al., 2008). The combined use of EEWS and structural control may reduce the structural vulnerability of specific systems, for example, critical buildings which have to be operable for emergency management purposes right after the event; e.g., hospitals, fire stations, or lifelines.

Currently, integration of structural control and EEWS relies substantially on semi-active devices. However, the key issue in the application of early warning to structural control is to account for the uncertainty in the estimation of the event's features the EEW is based on, because the efficiency of such systems depends on the quality of pre-arrival ground motion information provided.

In this paper, some very preliminary results related to a feasibility study about structural control integrated with *hybrid* EEWS (Iervolino et al., 2006), are presented and discussed. Although, interaction between earthquake early warning and structural control is a subject which still requires substantial investigation to be addressed.

## 2. Background

Recent efforts of real-time seismology on rapid assessment of earthquake magnitude and location enable to provide an estimate of the event's features from a few seconds to a few tens of seconds before the ground motion arrives at a specific site. Then, when an event is occurring, probabilistic distributions of magnitude and source-to-site distance are available. Consequently the prediction of the peak ground motion at the site (or spectral ordinates), conditional on the seismic network measures, may be performed in analogy with the well known probabilistic seismic hazard analysis (PSHA); e.g., Iervolino et al. (2006)

and Convertito et al. (2008). This results in time-dependent hazard curves which may be used as a support tool for automated decision making in order to reduce the expected loss of specific structures/infrastructures in the framework of performance-based earthquake engineering (PBEE), even in those cases where limited lead-time renders evacuation unfeasible. However, real-time peak ground motion predictions are performed in very uncertain conditions which both refer to the real-time estimation of source parameters and traditional uncertainties involved in PSHA.

### 2.1 RTPSHA

Seismologists have recently developed several methods to estimate the magnitude ( $M$ ) of an event given limited information of the P-waves for real-time applications. Similarly, the source-to-site distance ( $R$ ) may be rapidly determined by analyzing the time and order of the seismic stations detecting the developing earthquake. Therefore, it is possible to assume that, while the event is still propagating, estimates of  $M$  and  $R$  are available, and the peak ground motion at the site can be predicted via the probabilistic seismic hazard analysis conditional to the real-time information given by the seismic sensors network. In fact, assuming that at a given time  $t$  from the earthquake's origin, the seismic network can provide a vector of measures informative for the magnitude,  $\underline{\tau} = \{\tau_1, \tau_2, \dots, \tau_n\}$ , the posterior probability density function (PDF) of  $M$  conditional to the measures,  $f(m | \underline{\tau})$ , may be obtained via the Bayes theorem, as in Eq. (1):

$$f(m | \underline{\tau}) = \frac{f(m | \underline{\tau}) f(m)}{\int_{M_{\min}}^{M_{\max}} f(m | \underline{\tau}) f(m) dm} \quad (1)$$

In the Bayesian framework  $f(m)$ , the *a priori* distribution, is used to incorporate the information available before the seismic network performs the measurements. Then, in this application, a natural candidate for  $f(m)$  is the truncated exponential, derived by the Gutenberg-Richter relationship typically used in the

classic hazard analysis. The parameters  $\{\beta, M_{\min}, M_{\max}\}$  of Gutenberg-Richter relationship are dependent on the seismic features of the region under study and will be assumed for the Campania region equal to  $\{1.69, 4, 7\}$ .

The joint PDF  $f(\underline{\tau} | m)$  is the *likelihood* function. It is used to incorporate into the analysis all information on  $M$  contained into the real-time data. Under the hypothesis that the  $\tau$ -measurements are  $s$ -independent and identically distributed lognormal random variables it may be formulated as in Eq. (2).

$$f(\underline{\tau} | m) = \left( \frac{1}{\sqrt{2\pi}\sigma_{\ln(\tau)}} \right) \left( \prod_{i=1}^n \frac{1}{\tau_i} \right) e^{-\left( \frac{\sum_{i=1}^n (\ln(\tau_i))^2}{2\sigma_{\ln(\tau)}^2} \right)} e^{-\left( \frac{2\mu_{\ln(\tau)} \sum_{i=1}^n \ln(\tau_i) - n\mu_{\ln(\tau)}^2}{2\sigma_{\ln(\tau)}^2} \right)} \quad (2)$$

The parameters in Eq. (2) may be, for example, the mean,  $\mu_{\ln(\tau)}$ , and the standard deviation,  $\sigma_{\ln(\tau)}$ , of the log of the predominant period of the first four seconds of the P-waves retrieved from the study of Allen and Kanamori (2003), Eq (3). Combining Eq. (2) into Eq. 1, the posterior PDF of the magnitude results that of Eq. 4, which depends on the measures only via the summation of the logs,  $\hat{\tau} = \sum_{i=1}^n \ln(\tau_i)$  and  $n$ .

$$\begin{cases} \mu_{\ln(\tau)} = \frac{M - 5.9}{7 \log(e)} \\ \sigma_{\ln(\tau)} = \frac{0.16}{\log(e)} \end{cases} \quad (3)$$

$$f(m | \underline{\tau}) = \frac{e^{-\left( \frac{2\mu_{\ln(\tau)} \left( \sum_{i=1}^n \ln(\tau_i) \right) - n\mu_{\ln(\tau)}^2}{2\sigma_{\ln(\tau)}^2} \right)} e^{-\beta m}}{\int_{M_{\min}}^{M_{\max}} e^{-\left( \frac{2\mu_{\ln(\tau)} \left( \sum_{i=1}^n \ln(\tau_i) \right) - n\mu_{\ln(\tau)}^2}{2\sigma_{\ln(\tau)}^2} \right)} e^{-\beta m} dm} \quad (4)$$

Regarding the source-to-site distance, because of rapid earthquake localization procedures, a probabilistic estimate of the epicenter may also be available. For example, during an

earthquake, the algorithm developed by Satriano et al. (2008) allows to assign to each point of a grid, defined in the region where the network operates, the probability that the hypocenter is coincident with that point based on the sequence according to which the stations trigger,  $\underline{s} = \{s_1, s_2, \dots, s_n\}$ . Consequently, also the PDF of  $R$ ,  $f(r | \underline{s})$ , may be retrieved in real-time. Thus, it is possible to compute the probabilistic distribution (or hazard curve) of a ground motion intensity measure at a site of interest as in Eq. (5), which also requires an attenuation relationship,  $f(im | m, r)$ , available for the chosen IM. This procedure will be referred to as RTPSHA and may be used to predict, for example, of peak ground acceleration (PGA), Eq. (5), or spectral ordinates. The subscript ( $n$ ) in the left-hand side of Eq. (5) means that the computed hazard curve refers to a particular set of triggered stations and, therefore, evolves with time.

$$f_n(pga | \underline{\tau}, \underline{s}) = \int \int_{MR} f(pga | m, r) f(m | \underline{\tau}) f(r | \underline{s}) dm dr \quad (5)$$

When the hazard integral of Eq. (5) is computed (i.e., the prediction of the IM at the target site is obtained) the decision whether to issue an alarm or not is taken. The alarm issuance implies a decisional rule. For example, assuming that the predicted IM is the PGA, a simple one consists of issuing the alarm if the risk that the critical peak ground motion value ( $PGA_c$ ) will be exceeded in the strike, is larger than a probability threshold ( $P_c$ ), Eq. (6).

*Alarm if*

$$1 - \int_0^{PGA_c} f_n(pga) dpga = P[PGA > PGA_c] > P_c \quad (6)$$

For structural application of EEWS, the prediction of structural response in terms of an Engineering Demand Parameter (EDP), rather than in terms of a ground motion IM, may be of larger concern. This requires a further integration to get the PDF of EDP:

$$f_n(edp | \underline{\tau}, \underline{s}) = \int_{IM} f(edp | im) f_n(im | \underline{\tau}, \underline{s}) dim \quad (7)$$

where the PDF,  $f(edp | im)$ , is the probabilistic relationship between IM and EDP, and may be obtained, for example, via non-linear incremental dynamic analysis which was also developed for controlled structures (Barroso and Winterstein, 2002). Obviously, this approach can be extended further to predict the expected loss in a structure conditional on the measures of the seismic instruments, and this contains the highest level of information for alarm issuance decision (Iervolino et al., 2007).

### 2.2 ERGO: a prototypal EEW terminal.

RTPSHA above was implemented, in a simplified form, in ERGO (EaRly warninG demO) which is a visual terminal developed to test the potential of hybrid EEWs (Festa et al., 2009). The system was developed by staff of the RISSC lab ([www.rissclab.unina.it](http://www.rissclab.unina.it)) and of the Department of Structural Engineering of the University of Naples Federico II ([www.dist.unina.it](http://www.dist.unina.it)) under the umbrella of AMRA scarl ([www.amrcenter.com](http://www.amrcenter.com)). It was installed in the school of engineering of the University of Naples Federico II on July 25 2008 and continuously operates since then.

ERGO processes in real-time the accelerometric data provided by a part of the sensors of ISNet and it is able to perform the RTPSHA and eventually to issue an alarm in the case of events occurring with magnitude larger than 3 in the southern Appennines region. ERGO is composed of four panels (Figure 2):

#### 1. Real-time monitoring and event detection.

In this panel two kind of data are given: (a) the real-time accelerometric signals of the stations associated to the EEW terminal, shown on a two minutes time window; and (b) the portion of signal that, based on a signal-to-noise ratio determined the last trigger (i.e., event detection) for a specific station (on the left). Because it may be the case that local noise (e.g., traffic or wind) determines a station to trigger, the system declares an event ( $M$  larger than 3) only if at

least three station trigger within the same two seconds time interval;

#### 2. Estimation of earthquake parameters.

This panel activates when the first panel declares an event. If this condition occurs the magnitude and location are estimated in real-time as a function of evolving information from the first panel. Here the expected value of the magnitude as a function of time from the origin of the detected event and the associated standard error are given. Moreover, on a map where also the stations are located, it shows the estimated epicenter, its geographical coordinates and the origin time;

#### 3. Lead-time and peak-shaking map.

This panel shows the lead-time associated to S-waves for the propagating event in the whole region. As a further information, on this panel the expected PGA on rock soil is given on the same map. As per the second panel, this one activates only if an event is declared from panel 1 and its input information come from panel 2.

#### 4. RTPSHA and alarm issuance decision.

This panel performs RTPSHA for the site where the system is installed based on information on magnitude and distance from panel 2. In particular, it computes and shows real-time evolving PDFs of PGA at the site. Because a critical PGA value has been established for the site (arbitrarily set equal to 0.01 g) the system is able to compute the risk this PGA is exceeded conditional to the estimates for the ongoing event as a function of time. If such a risk exceeds 20% (i.e., the decisional rule of Eq. (6)) the alarm is issued and a otherwise green light turns into red. This panel also gives, as summary information, the actual risk that the critical PGA value is exceeded along with the lead-time available from the site and the false alarm probability.

Figure 2 refers to a real event detected and processed in real-time by ERGO on November

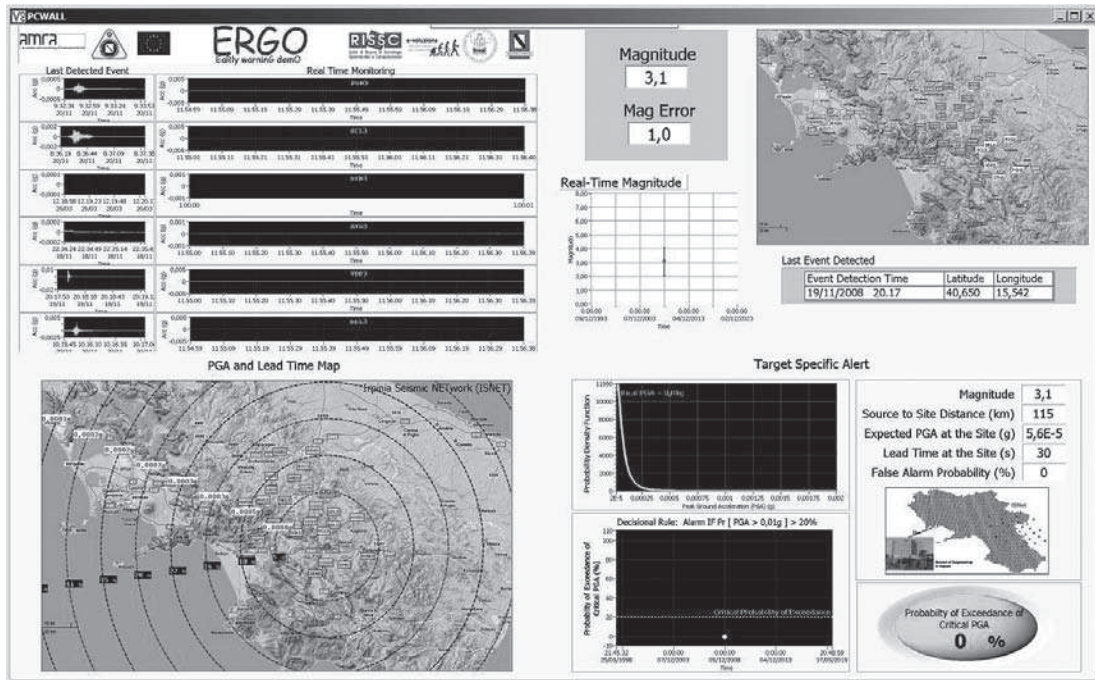


Figure 2: The ERGO EEW terminal

19 2008. The system estimated the event as a M 3.1 earthquake located close to Potenza (a town capital of the Basilicata region), with an epicenter 115 km far from the site. Because the event was a low-magnitude large-distance one, the risk the  $PGA_c$  could be exceeded was negligible and the alarm was, correctly, not issued. Finally, note that ERGO is a visual panel only for demonstration and testing purposes, but it may be virtually ready be connected to devices for real-time automated risk reduction actions.

### 3. EEWS and control systems for seismic protection of structures

The three major classes of control systems for protecting structures subjected to ground motion are: (1) *passive*, (2) *active*, and (3) *semi-active* (e.g., Symas and Constantinou, 1999; Soong and Spencer, 2002).

1. A passive control system is based on the motion of the structure (e.g., the relative motion within the passive device) to develop the control force, and does not require an external power source to operate. Such systems basically reduce the seismic

demand on the structure either increasing the energy dissipation potential and/or changing its fundamental oscillation period moving it away from the most energetic frequency content of ground motion (i.e., seismic base isolation). Note that when dealing with passive control, design usually means fixing a set of boundary conditions and choosing a device optimized for that set of conditions (in other words passive systems need to be designed according to an expected scenario of the seismic action). Then, it is hard to integrate EEWS with passive control systems.

2. An active control system supplies control forces based on feedback from sensors (located on the structure) that measure the excitation and/or the actual response. The recorded measurements from the response and/or excitation are monitored by a controller (a computer) which, based on an algorithm, operates the actuators producing the forces. The generation of control forces by electro-hydraulic actuators requires power sources on the order of tens of kilowatts for small structures and may

reach several megawatts for large structures. Active control strategies are based on information about the full waveform or structural response which can't be predicted by an EEWs, although *site-specific* EEWs (see Kanamori, 2005) may be potentially used to prepare the system when the earthquake is about to strike at the site of the structure.

3. A semi-active (SA) system develops control forces based on the feedback from sensors that measure the excitation and/or the response of the structure (Figure 3). However, the control forces are not realized, as in the active case, by actuators, but rather by modifying, in real-time and according to a preselected decisional rule, the mechanical characteristics of special devices (SA links). The energy required for the modification of the basic parameters of the devices is minimal, generally on the order of tens of watts, and may be furnished even by a simple battery (e.g., to open/close of a valve). Control strategies based on SA control combine the best features of both passive and active control systems offering the adaptability of active systems (without requiring the associated large power sources) and the reliability of passive systems. For these reasons, SA control strategies, seem to have a potential in seismic protection of structures and infrastructure in combination with an

EEWS. In fact, as shown in the following, for ON-OFF SA systems (i.e. SA system which can assume only two states of operation) the decisional rule (i.e. the decision of activating the control system) may be formulated on the basis of a single parameter representative of earthquake potential rather than the full waveform.

### 3.1 Fluid viscous dampers for EEW-based semi-active structural control

One means of achieving a semi-active damping device is to use a controllable valve to alter the resistance to flow of a conventional hydraulic fluid damper. Semi-active fluid viscous dampers typically consist of a hydraulic cylinder containing a piston head which separates the two sides of the cylinder. As the piston is cycled, the fluid within the damper (usually oil) is forced to pass through small orifices at high speeds. The pressure differential across the piston head, and thus the output force, is modulated by an external control valve which connects the two sides of the cylinder.

If the device is characterized by only two states (e.g., the valve can only be open or closed) the system is referred to as an ON-OFF SA system, otherwise if the mechanical parameter of the device can assume any value in a certain range (e.g. the valve opens and closes gradually) the system is referred to as a continuous SA system.

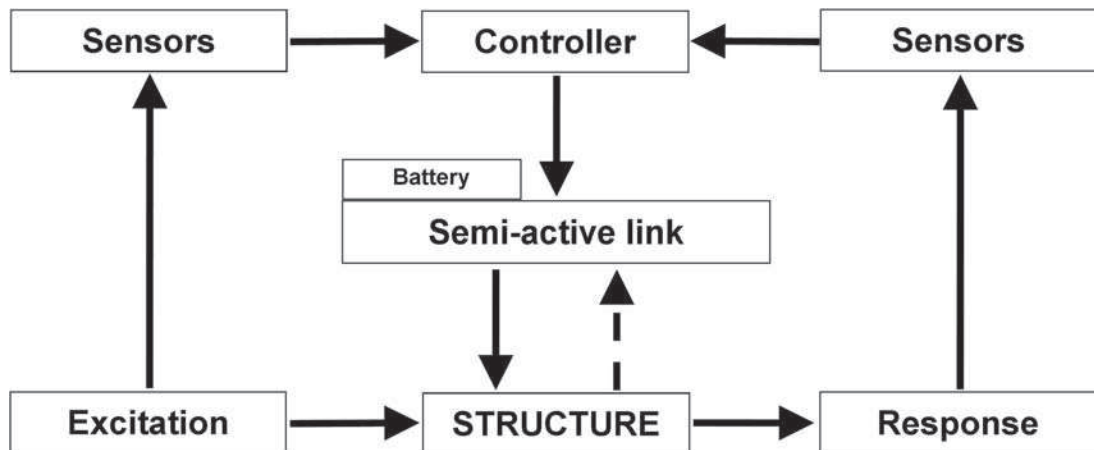


Figure 3: Block diagram of semi-active control systems (adapted from Soong and Spencer, 2002)

Although more complex models are available, the dynamic behavior of the fluid dampers over the frequency range of interest for structural control applications, may be described based on a simple phenomenological model consisting of a linear viscous dashpot with a voltage-dependent damping coefficient,  $C_{SA}(u)$ . The force output,  $F$ , is thus described by:

$$F = C_{SA}(u) \cdot \dot{x} \quad (8)$$

where  $\dot{x}$  is the relative velocity of the piston head with respect to the damper housing and  $u$  is the command voltage. The damping coefficient of Eq. (8) increases if the command voltage decreases and it is bounded by minimum and maximum values corresponding to the open and closed valve positions respectively, Eq. (9). The response time for modifying the variable damper from higher-to-low or low-to-high damping is generally less than 30 ms.

$$\begin{aligned} \text{valve closed} &\Leftrightarrow C_{SA}(u) = c_{\max} \\ \text{valve open} &\Leftrightarrow C_{SA}(u) = c_{\min} \end{aligned} \quad (9)$$

In the EEW prospective, once a prediction of a seismic demand parameter for a structure of interest is available, a decisional condition has to occur to issue the alarm (i.e. to activate the device). For example, the device may be activated if the expected value,  $E[EDP_{\text{uncontrolled}} | \underline{\tau}, \underline{s}]$ , of the structural response variable exceeds a critical threshold  $EDP_c$ , Eq. 10. The expected value of the chosen EDP may be computed as in Eq. (11) extending the RTPSHA concept.

$$\begin{aligned} C_{SA}(u) &= c_{\max} \quad (\text{i.e. Device ON}) \\ &\quad \text{if } E[EDP_{\text{uncontrolled}} | \underline{\tau}, \underline{s}] \geq EDP_c \\ C_{SA}(u) &= c_{\min} \quad (\text{i.e. Device OFF}) \\ &\quad \text{if } E[EDP_{\text{uncontrolled}} | \underline{\tau}, \underline{s}] < EDP_c \end{aligned} \quad (10)$$

$$E_n [EDP_{\text{uncontrolled}} | \underline{\tau}, \underline{s}] = \int_{EDP} \int_{IM} edp_{\text{uncontrolled}} f(edp_{\text{uncontrolled}} | im) f_n(im | \underline{\tau}, \underline{s}) dEDP dIM \quad (11)$$

#### 4. Example of basic interaction of EEWs and SA structural control

Let's consider a reference structure modeled as a  $T = 0.6$  s single degree of freedom (SDOF) system with an elastic-perfectly-plastic behavior and a yielding moment of 200 kNm. The structure may be representative of the simple one storey/bay frame in Figure 4a equipped with a bracing system including variable viscous dampers operating in ON-OFF SA mode. Similarly, the SDOF can describe a simple bridge with a deck free to move via rolling bearings at one side and constrained to the pier by additional devices in the other one (Figure 4b). In the uncontrolled configuration, the semi-active damper has the control valve fully open, and thus the damper produces no control force. In the controlled configuration, the control valve is held fixed in the closed position (i.e., in a high damping configuration).

The considered EDP related to structural damage is the interstorey drift ratio (IDR) as a function of the PGA. To get a relationship between IDR and PGA for the case-study structure incremental dynamic analysis (IDA) was carried

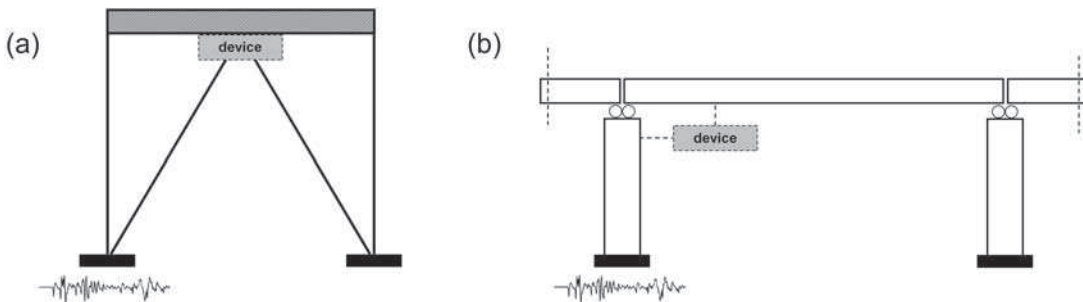


Figure 4: Examples of controlled structures which may be modeled as controlled SDOF systems

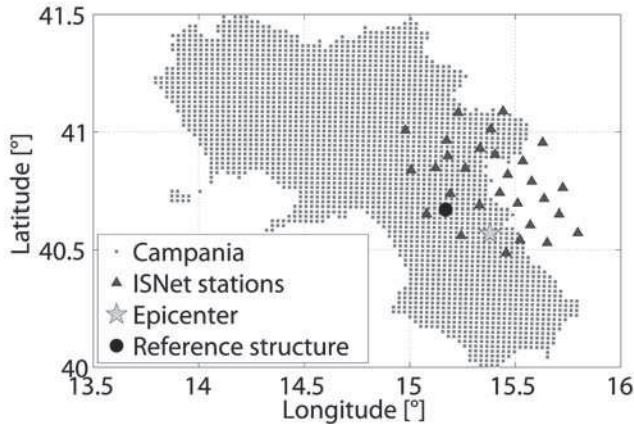


Figure 5: Scheme of the ISNet network and possible location of the reference structure

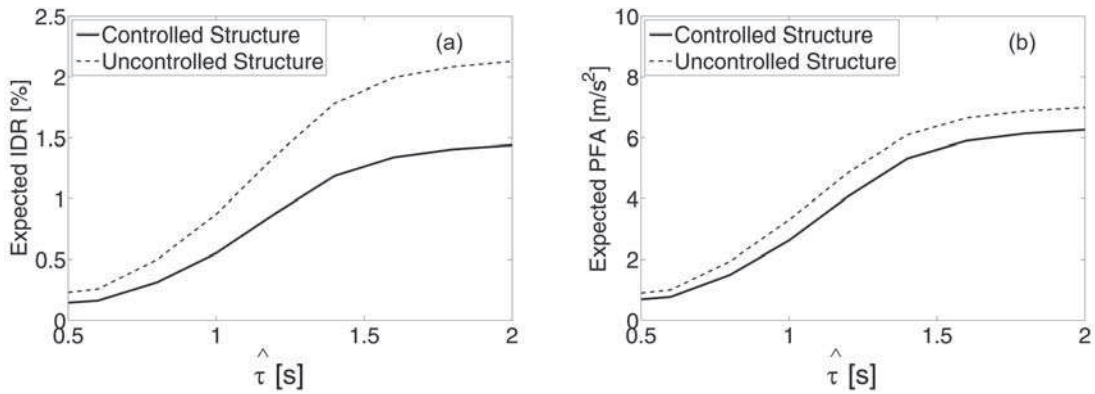


Figure 6: Comparison between the expected (a) IDR and the expected (b) PFA of controlled and uncontrolled structure as a function of the statistics of the network measurements

out (Vamvatsikos and Cornell, 2002). As an additional EDP, which may be of concern in the case one is interested in the response of non-structural elements, the peak floor acceleration (PFA) was also considered. Then, the (IDA) was also retrieved for the PFA as a function of the PGA<sup>1</sup>. Results in terms of IDR and PFA obtained by these simulations have been used to get a probabilistic representation of the seismic demand conditioned to the PGA, i.e. the PDF of Eq. (7) and Eq. (11).

The expected values of the chosen EDPs were computed via Eq. (11), as a function of the information provided in real-time by the EEWS ( $f_n(im | \underline{x}, s)$ ) was obtained by applying the methodology described in section 2.1). To this

aim it was supposed that the structure is in the Irpinia region at 10 km (in terms of epicentral distance) with respect to the location of an hypothetical earthquake occurring within the ISNet (Figure 5).

Note that Eq. (5) and consequently Eq. (11) depend on  $n$  (i.e., number of instruments of the seismic network have triggered and collected data). All the analyses are conditional to the fact that the level of information provided by the EEWS corresponds to 18 triggered stations out of 29 (i.e.,  $n = 18$ ); e.g., 18 measures of  $\tau$  are available. This is because, as shown in Iervolino et al. (2009), the information on the impending ground motion stabilizes when about 18 stations have provided  $\tau$  (i.e., the

<sup>1</sup> In order to obtain the relationship between the predicted PGA and the chosen EDPs in both controlled (damping ratio  $\xi = 15\%$ ) and uncontrolled case (damping ratio  $\xi = 5\%$ ), the non-linear structural model has been subjected to a set of 21 European ground motion records, each of those scaled to multiple levels of intensity between 0.1 g and 1 g.



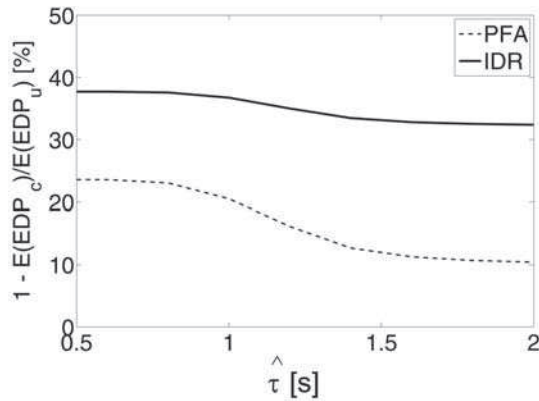


Figure 7: Response comparisons between the uncontrolled and controlled structure in terms of EDPs reduction as a function of the statistics of the network measurements

estimation of the PGA, and then of the EDP, does not benefit much from further information provided by additional ISNet stations). Moreover, since the localization method gives an about deterministic value of distance after 4 s for an event within the network, which is shorter than the time to trigger 18 stations, then the R value has been deterministically fixed to 10 km and, therefore, the relationship of the structural response with the information of the EEWS depends on  $\hat{\tau}$  only and does not depend on  $\underline{s}$ .

The expected values of both IDR and PFA were computed for 11 equally spaced values in the range between 0.5 s and 2 s as suggested by the relation between  $\hat{\tau}$  and the magnitude of an event in Allen and Kanamori, 2003. Results of the analyses are presented in Figure 6a and Figure 6b. The curves represent the trends of the EDPs for the specific structure at the given location. They provide the mitigation of structural response eventually given by the structural control (solid curves), with respect to the *as is* structure (dashed curves), in the case of different earthquakes represented by specific  $\hat{\tau}$  values and may be used for design of integrated EEWS and structural-control systems.

For the specific case-study, response comparisons between the uncontrolled and controlled structure shows that the peak acceleration and drift at the top floor may be reduced, on average, by about 15% and 35% respectively, if the EEWS triggers structural control<sup>2</sup> (Figure 7).

## 5. Conclusions

This paper presented a preliminary discussion about possible integration of state-of-the-art early warning systems (hybrid EEWS) and structural control. The issues associated to the real-time adaption of PSHA and PBEE for earthquake early warning purposes were given first. It was shown how the hazard integral can incorporate the information provided by a seismic network about a developing earthquake, and how it results in time-dependent hazard curves which may be used for automated decision making. A prototypal EEW terminal based on the seismic network (ISNet) installed in the Irpinia region in southern Italy was also presented.

Secondly, a procedure to compute the expected structural response in a EEW framework was discussed. The key element of the proposed procedure is the development, in real-time on the basis of the information provided by the EEWS, of probabilistic seismic demand curves for a structure equipped with semi-active control devices. These curves are a first attempt of tools aimed at the design of integration of structural control and earthquake early warning. Nevertheless, cost/benefit and loss analyses are still required to show the efficiency of such systems with respect to traditional control and seismic risk mitigation strategies for structures.

## References

Allen R. M., Kanamori H. (2003) The potential for earthquake early warning in southern California. *Science*, 300: 786–789.

<sup>2</sup> Results may change with location of the specific structure with respect to the earthquake.

- Barroso L. R., Winterstein S. (2002), Probabilistic seismic demand analysis of controlled steel moment-resisting frame structures, *Earthquake Engineering and Structural Dynamics* 31: 2049–2066.
- Convertito V., Iervolino I., Giorgio M., Manfredi G., Zollo A. (2008) Prediction of response spectra via real-time earthquake measurements. *Soil Dyn Earthquake Eng*, 28: 492–505.
- Festa G., Martino C., Lancieri M., Zollo A., Iervolino I., Elia L., Iannaccone G., Galasso C. (2009) ERGO: a visual tool for testing earthquake early warning systems. (in preparation).
- Kanamori H. (2005) Real-time seismology and earthquake damage mitigation, *Annual Review of Earth and Planetary Science*, 33, 195–214.
- Iervolino I., Convertito V., Giorgio M., Manfredi G., Zollo A. (2006) Real-time risk analysis for hybrid earthquake early warning systems. *Journal of Earthquake Engineering*, 10: 867–885.
- Iervolino I., Giorgio M., Galasso G., Manfredi G. (2009) Uncertainty in early warning predictions of engineering ground motion parameters: what really matters? *Geophysical research letters*, 36, L00B06  
doi:10.1029/2008GL0366449.
- Iervolino I., Giorgio M., Manfredi G. (2007) Expected loss-based alarm threshold set for earthquake early warning systems. *Earthquake Engn Struct Dyn*, 36: 1151–1168.
- Occhiuzzi A., Caterino N., Maddaloni G. (2008), Structural control strategies for seismic EWS, Proc. of 14<sup>th</sup> World Conference on Earthquake Engineering, Beijing, China, October 12–17 2008.
- Pnevmatikos N. G., Kallivokas L. F., Gantes C. J. (2002), Feed-forward control of active variable stiffness systems for mitigation hazard in structures, *Engineering Structures* 26: 471–483.
- Satriano C., Lomax A., Zollo A. (2008). Real-time evolutionary earthquake location for seismic early warning, *Bull Seism Soc Am*, 98: 1482–1494.
- Soong T. T., Spencer B. F. Jr (2002), Supplemental energy dissipation: state-of-the-art and state-of-the-practice, *Engineering Structures* 24: 243–259.
- Symas M. D., Constantinou M. C. (1999), Semi-active control systems for seismic protection of structures: a state-of-the-art review, *Engineering Structures* 21: 469–487.
- Vamvatsikos, D., and C.A. Cornell (2002). Incremental Dynamic Analysis, *Earthquake Engineering and Structural Dynamics* 31, 491–514.
- Weber E., Convertito V., Iannaccone G., Zollo A., Bobbio A., Cantore L., Corciulo M., Di Crosta M., Elia, L. Martino, C. Romeo A., Satriano C. (2007) An advanced seismic network in the southern Apennines (Italy) for seismicity investigations and experimentation with earthquake early warning. *Seism Res Lett*, 78: 622–634.